JOURNAL OF MATERIALS SCIENCE 20 (1985) 3949–3956

Microstructural, etching and hardness studies on flux-grown $KNiF_3$ crystals

P. N. KOTRU, SUCHETA GUPTA, S. K. KACHROO
Department of Physics, University of Jammu, Jammu 180001, India
B. M. WANKLYN
Department of Physics, Clarendon Laboratory, University of Oxford, UK

Surface structures on {1 0 0} faces of flux-grown $KNiF_3$ crystals are reported. Etching experiments establish HNO_3 to be a dislocation etchant for the crystals. The etching behaviour of the HNO_3–$KNiF_3$ surface system is investigated. The results obtained on the effect of etching time and etchant concentration on lateral extension and depth of dislocation etch pits are reported. It is observed that the etchant is rendered passive after some period of initial etching. Indentation-induced hardness testing studies suggest a Vickers microhardness value in the range of (2.93 to 3.50) $\times 10^2 kg\,mm^{-2}$, and the response of indentation to load is in accordance with Kick's Law.

1. Introduction

The potassium transition metal fluorides of composition KMF_3(M = Fe, Co or Ni) have attracted considerable attention on account of their magnetic properties. They have a cubic perovskite structure at room temperature and become antiferromagnetic above liquid nitrogen temperature. As they are good examples of simple Heisenberg magnets, large crystals are required for a variety of magnetic measurements [1]. Flux growth has the advantage of yielding crystals with habit faces, which makes them suitable for microtopographical studies. This type of study is particularly important, because in the case of the flux-growth technique one does not know exactly what happens while the crystal is growing, on account of high temperature involvement. Thus there is no alternative but to use indirect means, such as microtopographical studies, to obtain information concerning growth mechanisms and the dissolution process. In this respect flux-grown $KNiF_3$ crystals are no exception, because growth of these crystals involves very high temperatures and the growing system remains sealed.

The mechanical properties of solids are studied through their response to inhomogeneous stresses resulting from concentrated loading. These tests are easier to perform than tests involving uniform axial stresses. For example, concentrated loading requires only a small surface area which can be prepared comparatively easily [2].

In the present paper, the authors report the results of microtopographical investigations, etching and indentation-induced hardness testing studies on {1 0 0} faces of flux-grown $KNiF_3$ crystals. To the best of the authors' knowledge, there is no such report on microtopography, etching and mechanical properties of these crystals.

2. Experimental details

The flux growth of $KNiF_3$ has already been reported in the literature [3, 4]. $KNiF_3$ crystals used in the present study were prepared using growth conditions as reported by Wanklyn [4]. The grown crystals are cleaned in dilute HNO_3 to separate the crystals from the flux. The surface of "as-obtained" crystals were thoroughly cleaned and then coated with the optimum thickness of thin films of silver in a high-vacuum coating plant, to enhance their contrast. The crystal surfaces were then studied under a

0022–2461/85 $03.00 + .12

universal metallurgical microscope (Neophot–2, Carl Zeiss, Germany). Up-to-date means of optical investigation such as multiple beam interferometry [5], light profile [6] and phase contrast microscopy [7] were also employed wherever necessary.

Samples approximately 4 mm × 2 mm × 1.5 mm in size were used for microhardness studies. All the measurements were carried out at room temperature (30° C) using a Vickers microhardness tester mhp100 attached to the above-mentioned microscope. After proper mounting and cementing, the selected surfaces were indented for various loads ranging from 10 to 100 g, keeping the time of indentation at 2 sec. The distance between any two consecutive indentation marks was kept greater than eight times the diameter of the indent mark. This was done to ensure that surface effects were independent of one another. The diameter of the indent mark was determined by the filar eye-piece with a least count of 0.25 μm ($\times$ 500). The value of microhardness is calculated using the expression $H = 1.8544 \times P/d^2\,\mathrm{kg\,mm^{-2}}$, where P is load applied in grams and d the diagonal length of the indenter impression in micrometres. Etching experiments were also performed using HNO_3 of different concentrations.

3. Observations

3.1. Surface structures on as-obtained crystals

Usually {1 0 0} faces of $KNiF_3$ crystals show evidence of having been subjected to the process of dissolution. The dissolution appears in the form of selective etching. The following patterns were observed.

3.1.1. Isolated etch pits and rows of etch pits

Practically every {1 0 0} face that was examined showed the presence of etch pits, although their density differed in different cases. Some regions were so densely etched that it was very difficult to estimate the dislocation density accurately. Interferometric examination revealed that the depths of etch pits vary between 0.5 and 20 wavelengths of green light. Fig. 1 shows part of a {1 0 0} face showing parallel rows of square etch pits. The etch pits are arrayed in rows strictly oriented in the [0 0 1] direction. These parallel rows of etch pits appear to have developed along slip traces [1]. Under suitable conditions of etching, a small-angle grain boundary would appear as a row of discrete etch pits. Fig. 2 shows an etch pattern on an as-obtained crystal. One observes rows of

Figure 1 Parallel rows of square etch pits in the [0 0 1] direction along slip traces on {1 0 0} faces.

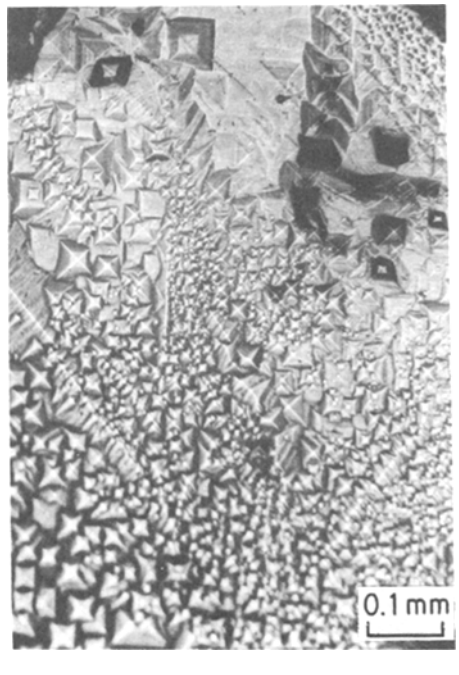

Figure 2 Equidistantly spaced etch pits along grain boundaries in combination with densely populated etch pits.

uniformly spaced etch pits. It is conjectured that the rows of etch pits observed represent grids of parallel dislocations caused by small-angle grain boundaries. Intersecting grain boundaries were also observed on the crystal surface. Such uniformly spaced etch pits were observed on a number of crystals.

3.1.2. Twin boundaries

Usually square-shaped etch pits observed on as-obtained {1 0 0} faces of $KNiF_3$ crystals are strictly oriented as shown in Fig. 1. This is bound to be the case if the surface is that of a single crystal. If, however, the crystal is twinned, the etch pits may either be differently shaped or differently oriented on the two sides of the boundary separating the twinned grains. It is, however, difficult to judge the change in orientation of square etch pits unless the difference in orientation of twinned grains is different from 90° or its integral multiple. Fig. 3 shows two well-demarcated regions on a {1 0 0} face. One can also observe that the morphology of growth bands in the two regions (A and B) is different. It appears that the two regions belong to two crystals which are in a twinned relationship. The growth bands in Region A originate somewhere from a corner in the lower left region of the photomicrograph. Safa *et al.* [1], during X-ray topographic investigations, observed similar growth bands and noted that at all times growth occurred at equal speeds on {1 0 0} faces. Such growth bands arise from variation in the crystal lattice parameter during growth. Such changes may be produced by temperature gradients which result in changes in patterns of convective flow in the melt adjacent to the crystal surface. This results in very small changes in composition in the deposited layers of the crystal, probably with ions of the flux incorporated substitutionally in the lattice. Our observation confirms the presence of growth bands and also that at all times growth occurred at equal speeds.

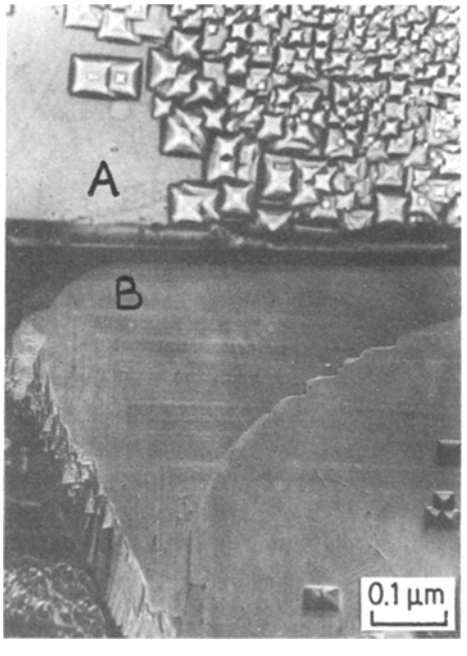

Figure 3 Well-demarcated regions on a {1 0 0} face showing the difference in the density of etch pits. Notice the difference in morphology of growth bands in the two regions (case of a twinned crystal).

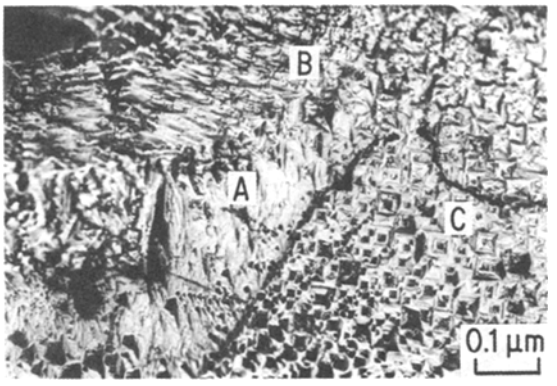

Figure 4 Etch patterns on a {1 0 0} surface delineating three regions A, B and C twinned with respect to each other. Notice the change in the shape and orientation of etch pits.

Fig. 4 is an interesting case of twinning showing three regions A, B and C which are twinned with respect to each other, as could be suggested by the etch patterns exhibited by the surface.

3.1.3. Irregular structures and microdiscs

Fig. 5 is a photomicrograph illustrating impurities attached to the host surface of $KNiF_3$ crystals. The impurities appear in the form of wide ridges of various lengths on the surfaces. The structure of one portion of a ridge is shown at higher magnification in Fig. 6. Interferometric studies have confirmed that these ridges are elevations of different heights. These inclusions have not been washed out during the time the crystals received etching as a result of the cleaning process. These inclusions could be any flux material or impurity in the starting material, which is getting phased out at almost the

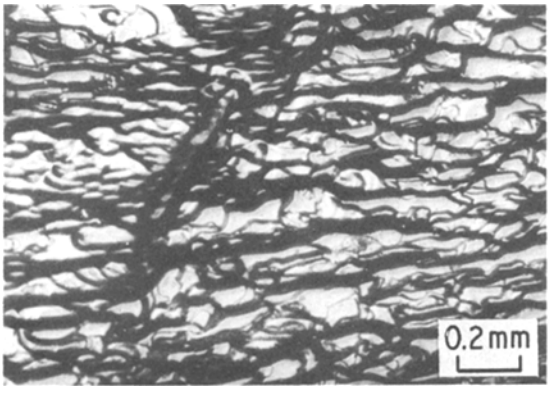

Figure 5 Impurities in the form of wide ridges of various lengths on a {1 0 0} surface.

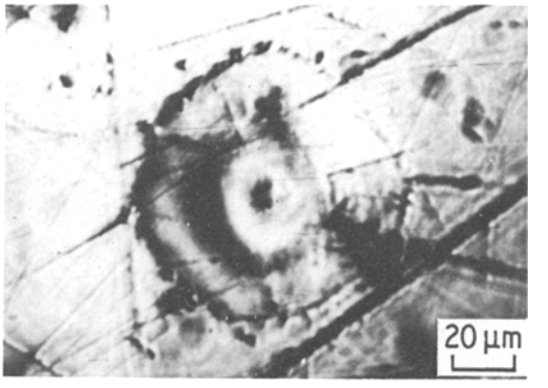

Figure 7 Elevated disc patterns indicating their origin due to the covering process of impurities.

cessation of crystal growth. Elevated microdisc patterns have also been observed on surfaces. These microdiscs, when examined at higher magnification, indicate some irregular features on their surfaces. An important question arises as to what has led to the formation of such microdiscs. Although the impurities have been observed in the form of ridges, there is a chance that during growth these impurities may also get attached to the crystal surface in the form of spherulites or rosettes. These impurities, if attached to the host surface before growth has ceased, are bound to affect the advancement of growth fronts. The advancing growth fronts may also envelop these impurities (if their attachment took place long before the cessation of growth) and incorporate them into the crystal as impurities. Such a covering process of impurities by growth fronts may also lead to the formation of elevated features on the surface,

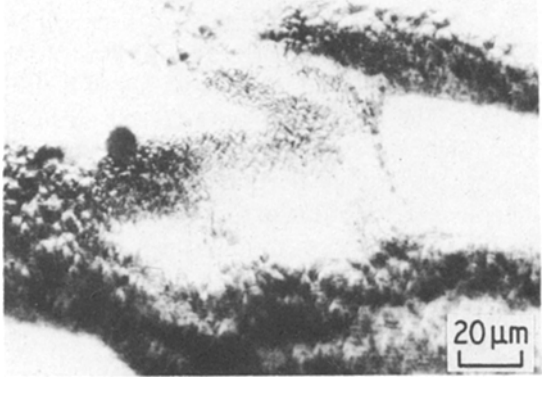

Figure 6 Protrusions of Fig. 5 at a higher magnfiication, showing them as aggregates of impurities.

which could possibly be in the form of discs. It is conjectured that the formation of microdiscs shown in Fig. 7 may be attributed to this mechanism, while Figs. 5 and 6 are the cases where the attachment of impurities took place after the cessation of growth.

3.2. Etching experiments

Most of the as-grown (flux-cleaned) $KNiF_3$ crystals studied during the present investigation exhibited etch patterns on their surfaces as already shown. It is possible that the flux-cleaned crystals were etched in the cleaning process when the crytals were placed in HNO_3 for cleaning and separation from flux. The experiments performed on etching of $KNiF_3$ crystals in HNO_3 indicate a similarity in shape and orientation of etch pits thus produced with those which result from the cleaning process on as-obtained crystals. The results are in favour of an argument that the cleaning process is the source of etch patterns on as-obtained crystals. In order to study etching behaviour in the HNO_3–$KNiF_3$ surface system some experiments were performed. Two types of regions of a crystal surface were selected for etching experiments, one which already had etch pits due to the cleaning process (referred to as "old pits" from now on) and others which did not have etch pits. Freshly nucleated pits at such sites will be referred to as "new pits".

3.2.1. Variation of lateral extension and depth with time of etching

Figs. 8a and b respectively show the dependence of lateral extension (taken as an average of

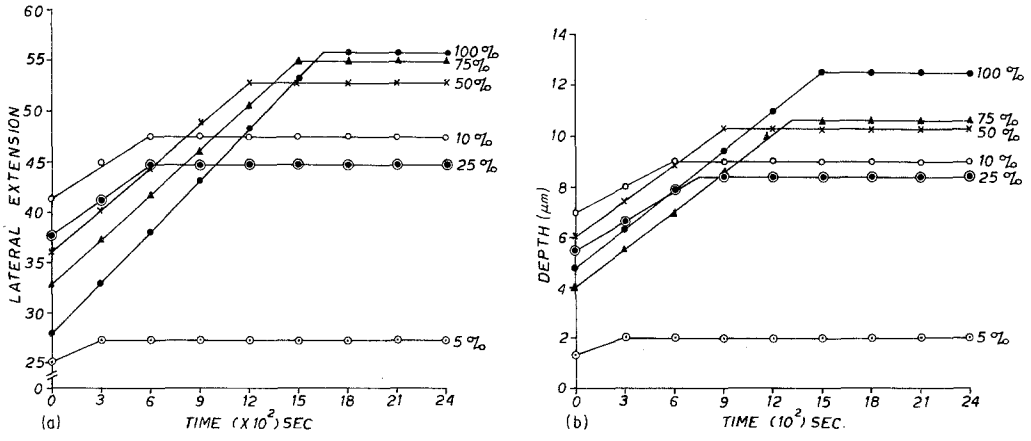

Figure 8 Graph showing variation of (a) lateral extension and (b) depth with time at different concentrations of the etchant at 30° C.

length and breadth) and depth of new (freshly nucleated) etch pits on time with different concentrations of the etchant in the range 5 to 100% at room temperature (30° C). It is significant to note that after some etching, the etchant ceases to attack in each case of Fig 8a or b. However, the time of attainment of inactivity by the etchant is different at different concentrations; in general, the higher the etchant concentration, the longer is the time during which it acts. In other words, with the decrease in etchant concentration from 100 to 5%, the time of initiation of inactivity of the etchant also decreases, whether it be along the surface (lateral extension) or perpendicular to the surface (depth). Identical behaviour in the HNO_3–$KNiF_3$ surface system is exhibited in the case of etching of old pits. In this regard the behaviour of the system is identical, whether the surface has a previous history of preferential etching or not. Such behaviour of the etchant is attributed to the phenomenon of passivity [8, 9]. Kotru *et al.* [10] have reported that for the $LaAlO_3$–HNO_3 system, the etchant is rendered inactive when boiling 100% HNO_3 is used. In this regard, the behaviour in the $KNiF_3$–HNO_3 system shows a different response so far as the passivity of the etchant is concerned.

3.3. Microhardness measurements

Indentation-induced hardness testing studies have been carried out in the load range 10 to 100 g. Plane surfaces were chosen for indentation purposes. It is observed that the size of the indenter impression increases as the load increases, implying a decrease of hardness with increasing load. For example, the impression obtained on {1 0 0} faces of $KNiF_3$ crystals after indenting with 20 and 100 g are shown in Figs. 9a and b. Davison and Vaughan [11] have shown that the size of the dislocation rosette produced around a microhardness indentation is a useful and convenient test for determining the mechanical strength of single crystals. The deformation pattern around the indentation on the present samples was revealed by etching the crystal in an etchant (50% HNO_3 for 20 min). It is found that the arm lengths which correspond to distances travelled by the dislocations decrease as the microhardness increases (i.e. as the load decreases), as is shown by examples offered by Figs. 9c and d. Further etching of the same surfaces (50% HNO_3 for 20 min) of Figs. 9c and d maintained the same arm length, though etched more deeply, as is shown in Figs. 9e and f. The thickening of the pattern is because of repeated preferential etching along the strain pattern due to indentation.

Table I gives Vickers hardness numbers (VHN) for {1 0 0} faces of $KNiF_3$ crystals at

TABLE I Microhardness measurements

Load, P(g)	Vickers Hardness Number (kg mm^{-2})
10	350 . 189
20	331 . 707
40	315 . 589
60	299 . 478
80	296 . 006
100	293 . 922

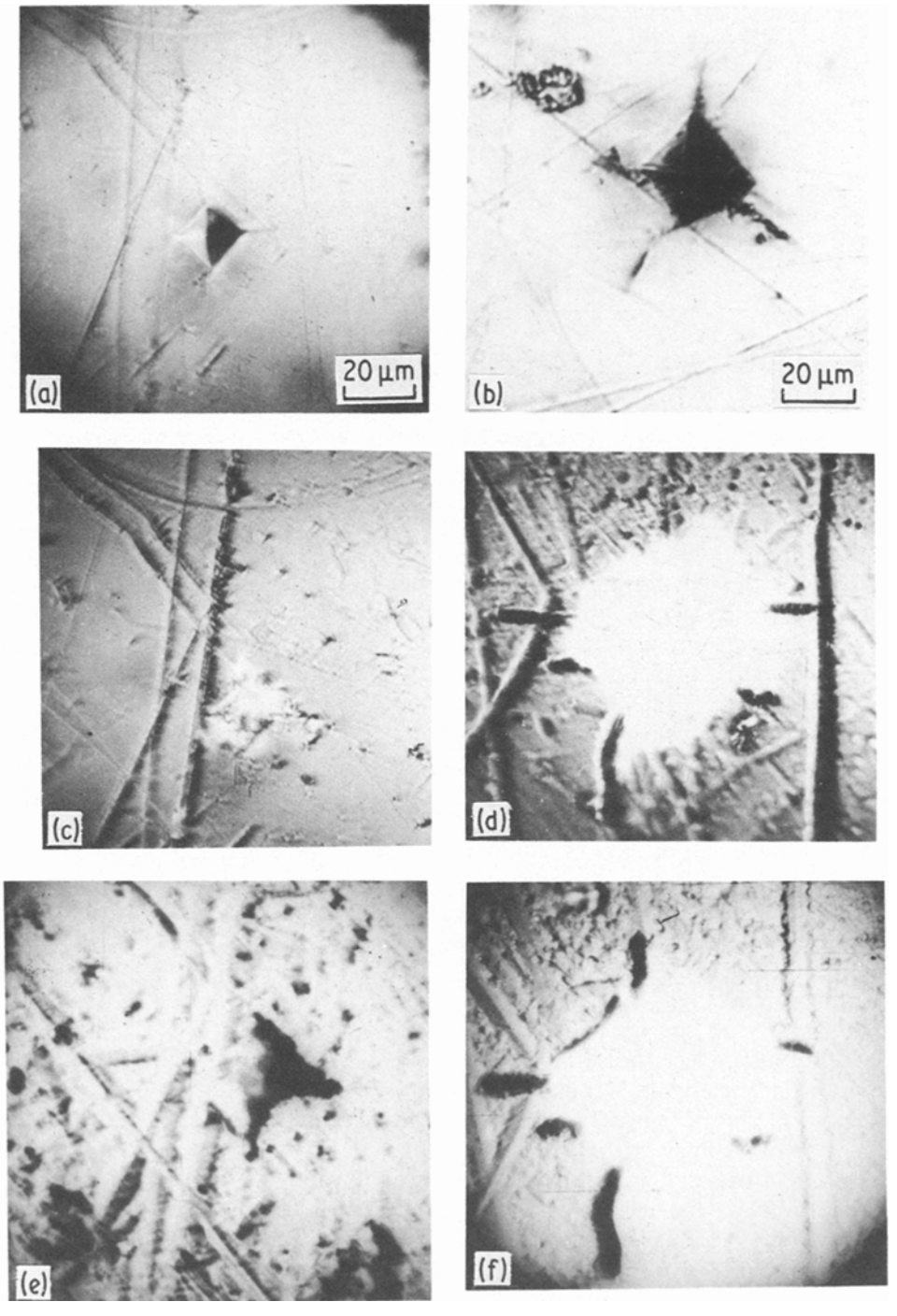

Figure 9 Indenter impression on a {1 0 0} face showing strain patterns with a load of (a) 20 g, (b) 100 g. (c, d) Corresponding deformation patterns around the indentation marks of (a, b) revealed after 20 min of etching in HNO_3. Notice the dislocation rosette pattern, deep etching at the indentation site, and increase in arm lengths of the pattern as the load increases. (e, f) Deformation patterns of (c, d) after further etching of 20 min in HNO_3 revealing deeper etching at the indentation mark and along the arms of rosette patterns, without any further increase in the arm lengths.

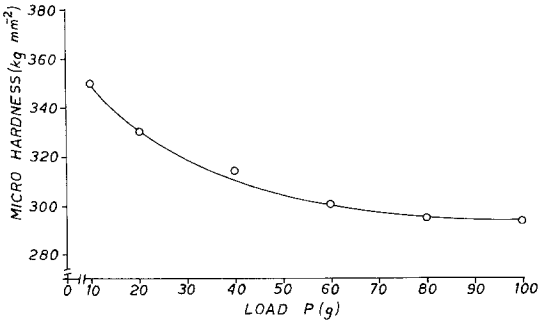

Figure 10 Graph showing dependence of microhardness number on load.

different loads. The dependence of microhardness value on load is depicted in Fig. 10. The variation shows the decrease of microhardness up to a load of 80 g, after which it remains almost constant. The indentation response to load is in accordance with Kick's law, $P = K_1 d^n$, where P is the applied load in grams, K_1 is the standard hardness, n is the constant and d is the diameter of the impression in micrometres. Kick's analysis of hardness postulate a constant value of $n = 2$ for all geometrically similar impressions. This equation was further supported by Schultz and Henemann [12] by proposing that Vickers hardness and microhardness values were comparable. However, the above law did not receive wide acceptance on account of the fact that n is usually not found to be 2 [13]. Kotru *et al.* [14] have also found $n < 2$ for rare-earth perovskites and found their results strictly in accordance with the modified law, known as Hays and Kendall's law [15], $P - W = K_1 d^n$, in which the concept of a material's resistance pressure, W, is taken into consideration. According to this modified law, when load P is applied to a crystal sample it is partially affected by a smaller resistance pressure W, which is a function of the material under testing. In the case of rare-earth perovskites investigated by Kotru *et al.*, [14], the value W was reported to be of the order of 10^{-4} kg. In the present case, when $\log P$ is plotted against $\log d$ (Fig. 11) it is a straight line. The slope of the curve yields $n = 2$.

The only possible explanation for the validity of Kick's law in the case of $KNiF_3$, unlike that of rare-earth perovskites reported by Kotru *et al.* [14], is that the value of resistance pressure offered by the former may be of a very low order and hence negligible. A negligible value of W would reduce the modified law of Hays and Kendall to that of Kick's law. Thus the results reported in this work show that Kick's law of microhardness is applicable to $KNiF_3$ crystals. In this respect, the results reported by Saraf [13] for untreated samples of barite crystals are significant. He reported n to be of the order of 2 only, but to attain values greater than 2 when the load is increased beyond 10 g. The graph of $\log P$ against $\log d$, as reported by him, does not yield a single straight line but two straight lines of different slopes meeting at a kink, which is obtained at a load of 10 g.

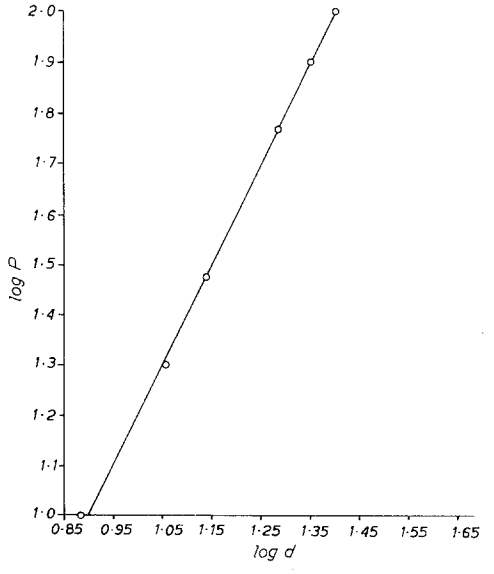

Figure 11 Graph of log P against log d, yielding a straight line with slope $n = 2$.

4. Conclusions

(a) During the growth of $KNiF_3$ crystals by the flux technique, impurities get phased out from the solution and get attached to the growing $KNiF_3$ crystal surfaces. The attached impurities give rise to typical forms of surface structures on the crystals.

(b) Most of the $KNiF_3$ crystals show evidence of having received etching during their cleaning operations in HNO_3.

(c) Besides isolated dislocations, planar defects like low-angle grain boundaires and twin boundaries are present in $KNiF_3$ crystals.

(d) With a decrease in etchant concentration from 100 to 5% at 30° C, the time of onset of passivity decreases for the HNO_3–$KNiF_3$ surface system.

(e) The microhardness values fall in the range of (2.93 to 3.50) $\times 10^2 \text{kg mm}^{-2}$. The hardness decreases upto a load of 80 g, after which it remains almost constant. The indentation response to load is in accordance with Kick's law.

Acknowledgements

One of us (S.K.K.) is grateful to the University Grants Commission for the award of a Junior Research Fellowship. The authors are grateful to Dr G. Garton, Head of the Crystal Growth Group, Clarendon Laboratory, University of Oxford, for his encouragement in the collaborative research programme between the Physics Department, University of Jammu and his laboratory. The authors are also grateful to Professor Y. Prakash, head of the Physics Department, Jammu University for his interest and co-operation.

References

1. M. SAFA, B. K. TANNER, B. J. GARRARD and B. M. WANKLYN, *J. Cryst. Growth* **39** (1977) 243.
2. C. L. SARAF and J. R. PANDYA, private communication (1970).
3. B. M. WANKLYN, *J. Cryst. Growth* **5** (1969) 279.
4. *Idem, J. Mater Sci.* **10** (1975) 1487.
5. S. TOLANSKY, "Multiple Beam Interferometry" (Oxford Univesity Press, Oxford, 1947).
6. *Idem, Z. Electrochem.* **56** (1952) 263.
7. A. H. BANNET, H. OSTERBERG, H. JUPNIK and O. W. RICHARDS, "Phase Microscopy" (John Wiley, New York, 1951).
8. G. MILAZZO, "Electrochemistry" (Elsevier, New York, 1963) p. 496.
9. B. BAKER, D. C. KOEHLER, W. O. FIECKENSTEIN, C. E. RODEN and R. SABIA, "Materials technology," Vol 2 (Prentice-Hall, Englewood, New Jersey, 1970) p. 217.
10. P. N. KOTRU, ASHOK K. RAZDAN, K. K. RAINA and B. M. WANKLYN, *J. Mater. Sci.* **20** (1985) 3365.
11. J. W. DAVISON and W. H. VAUGHAN, Report on Naval Research Laboratory Programme (April 1958).
12. F. SCHULTZ and H. HANEMANN, *Z. Metallkde.* **33** (1941) 124.
13. C. L. SARAF, PhD thesis, Maharaja Sayaji Rao University Baroda, India.
14. P. N. KOTRU, K. K. RAINA, S. K. KACHROO and B. M. WANKLYN, *J. Mater. Sci.* **19** (1984) 2582.
15. C. HAYS and E. G. KENDALL, *Metallography* **6** (1973) 275.

Received 2 November
and accepted 28 November 1984